nature materials
REVIEW ARTICLE
PUBLISHED ONLINE: 25 OCTOBER 2017 | DOI: 10.1038/NMAT5017

Towards properties on demand in quantum materials

D. N. Basov[1*], R. D. Averitt[2*] and D. Hsieh[3*]

The past decade has witnessed an explosion in the field of quantum materials, headlined by the predictions and discoveries of novel Landau-symmetry-broken phases in correlated electron systems, topological phases in systems with strong spin–orbit coupling, and ultra-manipulable materials platforms based on two-dimensional van der Waals crystals. Discovering pathways to experimentally realize quantum phases of matter and exert control over their properties is a central goal of modern condensed-matter physics, which holds promise for a new generation of electronic/photonic devices with currently inaccessible and likely unimaginable functionalities. In this Review, we describe emerging strategies for selectively perturbing microscopic interaction parameters, which can be used to transform materials into a desired quantum state. Particular emphasis will be placed on recent successes to tailor electronic interaction parameters through the application of intense fields, impulsive electromagnetic stimulation, and nanostructuring or interface engineering. Together these approaches outline a potential roadmap to an era of quantum phenomena on demand.

Quantum materials are on the ascent. This term embodies a vast portfolio of compounds and phenomena where ramifications of quantum mechanics are demonstrably real. Quantum materials are in the vanguard of contemporary physics in part because these systems afford an exceptional venue to uncover the many roles of symmetry, topology, dimensionality and strong correlations in macroscopic observables. Here we set out to explore the ways and means of creating new states of matter in quantum materials and manipulating their phases via external stimuli. Practical control of these properties is a precondition for exploiting quantum advantages in new photonic, electronic and energy technologies, a task of significant societal impact[1]. We will primarily focus on the following classes of quantum materials: transition metal oxides, Fe- and Cu-based high-T_c superconductors, van der Waals semiconductors, topological insulators and Weyl semimetals, and, finally, graphene.

The properties of quantum materials are anomalously sensitive to external stimuli. In these systems, interactions associated with spin, charge, lattice and orbital degrees of freedom are commonly on par with the electronic kinetic energy. A rather fragile balance between coexisting and competing ground states can be readily shifted via external stimuli, leading to a raft of quantum phases and transitions between them[2,3]. Furthermore, certain classes of driven quantum states (Fig. 1a and Box 1) are explicit products of coherent interaction between light and matter[4–6]. Alternatively, the properties of quantum materials can be pre-programmed by directly manipulating the electronic wavefunction and the attendant Berry phase that give rise to the anomalous velocity of electrons in a solid[7–9]. These complementary avenues of controls mean that investigations no longer need to be reduced to merely observing (in contrast, for example, to astrophysics). Instead, it is now feasible to attain, in a predictable fashion, 'properties on demand' by steering a quantum material towards a desirable ground, metastable or transient state.

Why properties on demand?

We outline some of the chief motivations behind the properties-on-demand approach in Fig. 1. First, time and again, discoveries of new states of matter stimulate disruptive advances in physics. For example, Floquet–Bloch states (Fig. 1a and Box 1, panel c), are a product of hybridization between intense optical pulses and surface states in Bi_2Se_3 crystals[10,11]. Replicas of the original electronic levels accompanied by energy gaps at avoided crossings in momentum space are an experimental signature of Floquet–Bloch states. The Floquet method enables control of both Landau symmetry breaking and topological phase transitions involving a change of a global topological invariant (for example, the Chern number).

Second, the properties-on-demand approach can help resolve longstanding enigmas. For example, experiments in high magnetic fields H offer innate advantages for addressing and settling some of the most pressing questions in high-T_c superconductivity: a problem that has eluded a thorough theoretical explanation[14]. Unresolved issues include the nature of the electronic state at $T > T_c$ from which superconductivity emerges, the character of the ground state as $T \to 0$ in the absence of superconductivity, and the origin of the quantum critical point (QCP): a zero-temperature phase transition where pressure or doping serve as tuning parameters (Fig. 1b). QCPs are firmly established in (antiferro)magnetic metals and were also observed in several classes of unconventional superconductors, including heavy fermion systems, organic materials and Fe-based pnictides[15]. Experimental access to the QCP in cuprates is difficult because this putative $T = 0$ transition is surrounded by a dome of superconductivity; however, the dome can be 'removed' in a high-H field. These experiments uncovered quantum oscillations (QO) of various transport properties as a function of the magnetic field strength[16]. QOs are a litmus test for the existence of a robust Fermi surface and of well-defined quasiparticles—concepts that early on were challenged in connection to high-T_c superconductors but are now nearly universally agreed upon.

[1]Department of Physics, Columbia University, New York, New York 10027, USA. [2]Department of Physics, University of California San Diego, La Jolla, California 92093, USA. [3]Department of Physics, California Institute of Technology, Pasadena, California 91125, USA. *e-mail: db3056@columbia.edu; raveritt@ucsd.edu; dhsieh@caltech.edu

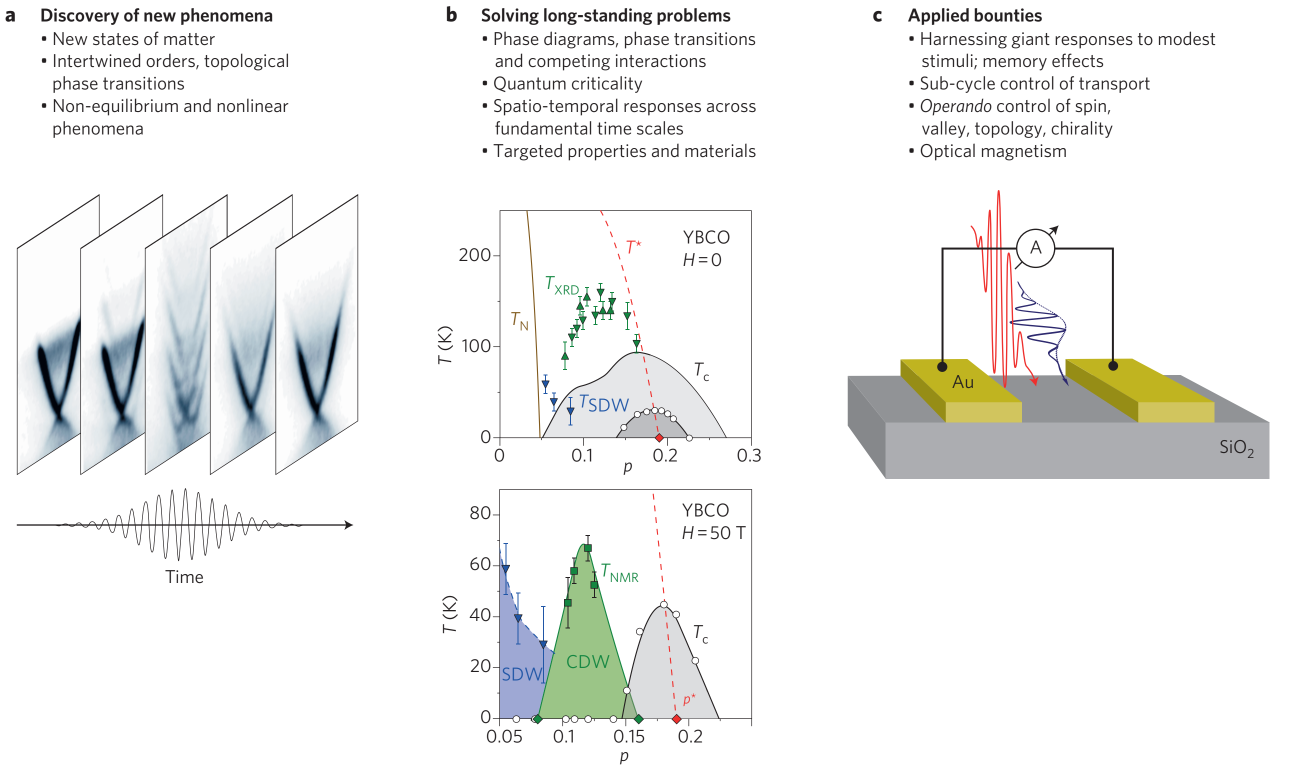

Figure 1 | The properties-on-demand approach. a, Photoexcitation of the surface states in Bi_2Se_3 crystals results in hybrid light–matter Floquet–Bloch states that manifest themselves as replicas of the original band structure. **b**, Phase diagram of a prototypical cuprate high-T_c superconductor $YBa_2Cu_3O_x$ (YBCO) in zero magnetic field (top) and in a magnetic field of 50 tesla (bottom). Grey domes depict the superconducting phase. CDW, charge density wave; SDW, spin density wave; NMR, nuclear magnetic resonance. T_{XRD} points display the onset of CDW modulations observed in X-ray diffraction data. **c**, Schematic of a metal–dielectric nanojunction. A few-cycle optical waveform reversibly increases the conductivity of amorphous SiO_2 by more than 18 orders of magnitude within 1 femtosecond, allowing electric currents to be driven, directed and switched by the instantaneous light field. Adapted from ref. 10, Macmillan Publishers Ltd (**a**); ref. 12, Macmillan Publishers Ltd (**b**); and ref. 13, Macmillan Publishers Ltd (**c**).

Third, alongside purely fundamental interests, the properties-on-demand strategy is pertinent in the quest to create devices based on new physical principles. For example, few-cycle optical pulses allow one to modulate the conductivity even in wide-bandgap insulators (Fig. 1c). Another actively pursued direction is to exploit anomalously strong responses to weak stimuli that are inherent to quantum materials. Fashioning a Mott transistor[17,18] is one example of this concept. Memory effects rooted in electronic/structural phase separation[19] and/or electronic correlations are closely related to quantum materials; memory effects are essential for the solid-state implementations of biologically inspired circuits[20] and may also facilitate energy-efficient computing. Yet another control route is provided by the Berry phase that underpins the tuning of topological conducting channels[7,8,21]. The same physics is essential for optical control of the valley degree of freedom in quantum materials with hexagonal lattices[22], including graphene and transition metal dichalcogenides (TMDs). Likewise, the chirality of both electronic and photonic[23,24] effects in quantum materials can be manipulated: chiral currents and propagating chiral hybrid light–matter modes known as polaritons can benefit from topological protection against backscattering[25–27]. Berry phase effects also underlie the phenomenon of 'shift currents'—an optically induced charge separation arising from asymmetry in the electronic wavefunctions—which provides a new paradigm for designing high-performance optical-frequency conversion and photovoltaic materials[28,29]. Recent studies of transition metal monopnictide-based Weyl semimetals (discussed in 'Topological phenomena under control') that exhibit the requisite band topology have revealed giant second-order nonlinear optical responses[30,31]. Another promising device concept is an optically pumped low-threshold laser based on a monolayer of the prototypical TMD material WSe_2[32]. Other emerging applications are discussed in the companion Review by Tokura *et al.*[33].

Ways and means of quantum control

In this section, we survey state-of-the-art methods (Fig. 2) that can be used to fine-tune a quantum material through its free energy landscape and briefly discuss the types of quantum phases that are accessible.

Static external perturbations. These offer the most controlled means of property tuning since thermal equilibrium is maintained throughout the process. Hydrostatic pressurization, typically applied using diamond anvil cells, is one approach that is commonly used to increase the orbital wavefunction overlap between neighbouring sites in a crystal, in turn increasing the ratio of kinetic (inter-site charge hopping) to potential (on-site Coulomb repulsion) energy. Pressure is often exploited to continuously tune a material across the Mott insulator-to-metal or even superconductor[34] phase boundary, which can be accompanied by an orders of magnitude resistivity change (Fig. 3a).

Heterostructuring. A large number of material parameters can be tuned by static perturbation of two-dimensional systems based on mechanically exfoliated nanoflakes or layer-by-layer epitaxy. Heterostructures offer pathways to induce energy gaps in the electronic structure by superlattice modulation, magnetic/superconducting proximity effects[35,36], or even to generate giant pseudomagnetic fields (>300 T) with substrate defects all giving rise to striking

Box 1 | Dressed states, hybrid quasiparticles and Berry phase engineering.

The tenet of dressed states is central to the physics of quantum materials. A familiar example of photon dressing (pictured, panel a) occurs as the result of light hybridization with dipole-active excitations in solids and is best revealed in the energy–momentum (E–k) dispersion. Polaritonic effects are especially rich in van der Waals atomic layers and crystals that support a full suite of these hybrid quasiparticles stemming from coupling to plasmons, phonons, excitions and magnons[57]. A high degree of confinement of polaritonic modes combined with relatively weak losses allows one to control and manipulate long-wavelength electromagnetic radiation at nanometre length scales.

Some of the most spectacular properties of quantum materials arise through many-body effects, a consequence of electrons strongly interacting with one another, with crystal lattice and/or with bosonic excitations. Landau asserted that quasiparticles in solids behave in many ways as free electrons, but with effective masses and velocities renormalized by interactions. The impact of renormalization is again most evident in the E–k dispersion: interactions impart a 'kink' at the bosonic energy scale (panel b). The kink separates low-energy coherent quasiparticles from incoherent states at higher energies. Femtosecond dynamics of these characteristics in cuprate high-T_c superconductors have helped to uncover the roles of spin fluctuations and the lattice in the formation of the modified dispersion[76,77].

Floquet quasiparticles are an example of an explicit product of light–matter interaction[4–6,10,11]. Under periodic electromagnetic excitation with frequency Ω (panel c), electronic bands become dressed, which manifests itself as a 'Floquet' copy of the original band shifted in energy by $\hbar\Omega$[61–65]. Even though the driving field oscillates at frequency Ω, crystals effectively rectify these oscillations, yielding a quasi-static dispersion on the timescale of the excitation pulse[65,78]. These photon-dressed electronic bands can overlap with other bands (left shaded region) and hybridize (right unshaded region).

Recent work has shown that non-trivial Berry phases can be engineered not just in bare electronic states but also in dressed states[4–6]. The basic mechanism involves hybridizing pairs of dressed bands (for example, with magnetic field or circularly polarized light) so that each acquires a non-trivial winding number, which produces protected edge modes (panel d). The finite Berry phase also modifies polaritonic dispersions. For example, the dispersion of edge plasmon-polaritons in graphene and TMD crystals is predicted to split into two distinct branches with opposite velocities[25–27]. The Berry phase can be conveniently controlled by photoexcitation suggesting entirely novel ways of attaining photoinduced responses.

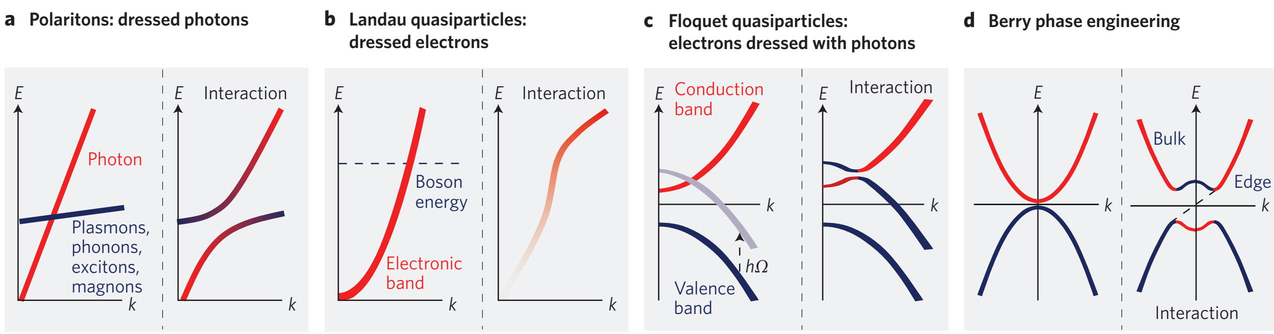

macroscopic consequences[37]. The recent surge in available families of van der Waals (vdW) materials[38], combined with the ability to produce nearly perfect interfaces between them, offers additional routes towards designing quantum phases by stacking vdW monolayers and controlling the coupling between them by the relative twist-angle misalignment. Electrostatic gating is readily attainable in vdW heterostructures and offers an additional degree of control over these materials. For example, electrostatic tuning of a high-mobility electron liquid in graphene allows one to select the regime of carrier density when the flow of electrons becomes viscous, whereas electric conductance can exceed the limits of ballistic transport[39]. Oxide heterostructures have also enabled the stabilization of interesting electronic phases at the interfaces of dissimilar oxides[40] or via interactions with the substrate. A recent example of the former is the implementation of a polar metal: a novel form of a conducting material with a static microscopic polarization at equilibrium[41].

High magnetic (B) fields. Another route to directly manipulate the electronic degrees of freedom in a material is the use of external magnetic fields. Well-known consequences include the collapse of dispersive electronic bands into cyclotron orbits or reorientation of ordered magnetic moments, all occurring without necessarily altering the lattice structure. The relevant energy scales are set by the cyclotron energy $\hbar\omega_c \sim \hbar eB/m$ and/or Zeeman energy $E_Z \sim g\mu_0 B$ (where e is the electron charge, m is the electron mass, g is the electron gyromagnetic ratio and μ_0 is the Bohr magneton), which can reach a few meV in fields of order 10 T. The integration of high magnetic fields with accelerator-based light sources including synchrotrons and free electron lasers now allow for spectroscopic interrogation of B-field induced phase transitions such as those between high-T_c superconducting and charge density wave ordered phases[42]. With the advent of pulsed magnet technology, fields exceeding 100 T ($\hbar\omega_c$ and E_Z in the tens of meV range), have recently been achieved, opening up new regions of complex material phase diagrams[43].

High electric field perturbation and stimulation. Advances in sub-picosecond pulsed lasers allow for quantum materials to be strongly driven and characterized by impulsive electromagnetic stimulation on the fundamental timescales of electronic and atomic motion (Fig. 2). For example, intense THz fields[44] in the range 10^6–10^7 V cm^{-1} can be generated across a broad swath of the electromagnetic spectrum to drive quantum phases at their natural energy scales. The electric field can be further enhanced by integrating quantum materials with metamaterials[45]. The strength of the perturbing electric field is a key enabler in dynamic materials control research. For example, strong, high-frequency fields can initiate phase transitions, including the insulator-to-metal transition[45] (discussed in 'Revealing hidden phases and new states of matter') or drive nonlinear effects such as on-resonance parametric amplification and high harmonic generation[46,47]. Sub-gap electromagnetic

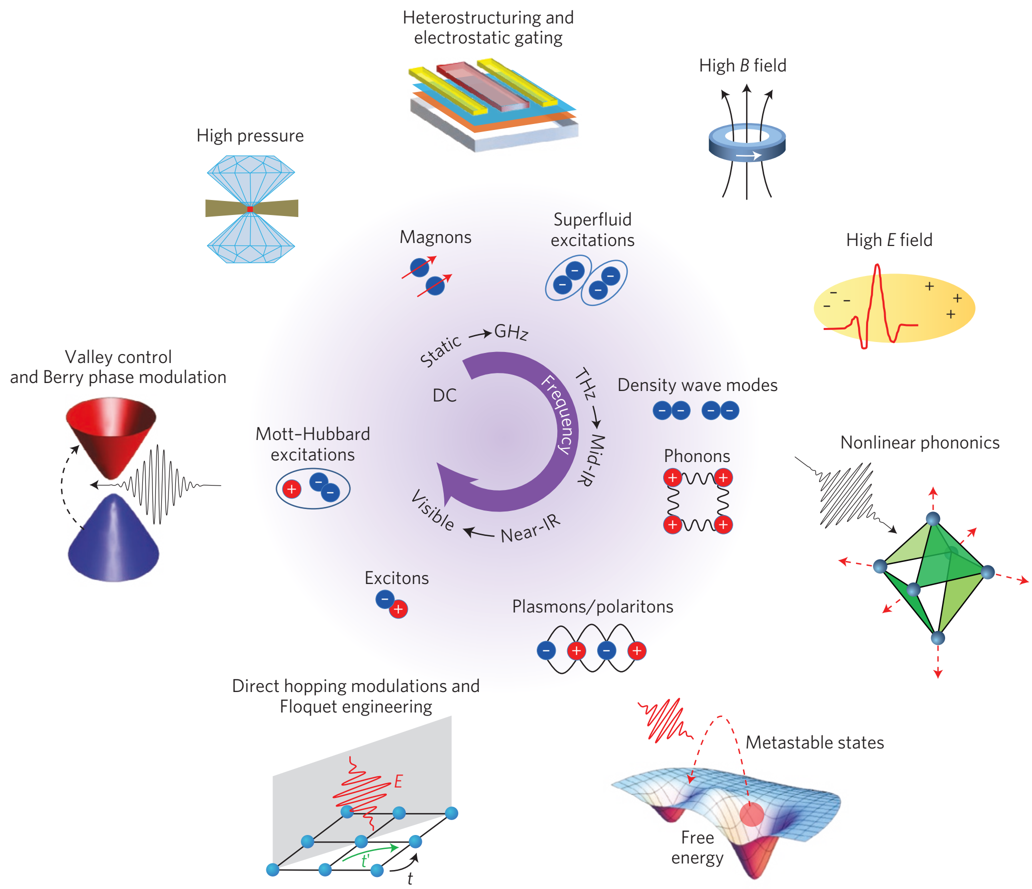

Figure 2 | Methods for controlling quantum phases. Elementary excitations in quantum materials and select control techniques arranged (clockwise) in order of ascending frequency.

excitation can be characterized in terms of the Keldysh parameter, $\gamma = a\sqrt{2mE_g}/\hbar\varepsilon$, where a is the lattice spacing, m the carrier mass, E_g the bandgap, and ε the Floquet parameter (given as $\varepsilon = eaE/\hbar\omega$, where E is the electric field and ω the frequency). Tunnelling dominates for $\gamma < 1$, while multiphoton absorption dominates for $\gamma > 1$. For sufficiently high fields (1–10 MV cm^{-1}) at THz and mid-infrared frequencies, the tunnelling regime ($\gamma < 1$) is operative, resulting in novel phenomena and unexpected effects such as massive population transfer between bands far in excess of the photon energy (that is, $E_g \gg \hbar\omega$)[44,48,49]. An exciting research direction that will remain outside of the scope of this Review is the electrical and optical control of magnetism[50,51].

Nonlinear phononics. Light-induced lattice displacements can in principle change the symmetry of a material and significantly alter its free-energy landscape, leading to new, low-energy quantum states. Specifically, mid-infrared pulsed excitation of infrared-active phonons has been utilized to impart and/or to relieve net structural distortions. This novel method, dubbed nonlinear phononics, capitalizes on coherent coupling between light and lattices. The lattice is altered by the oscillating field due to anharmonic coupling between infrared and Raman-active modes[52,53]. Spectacular photoinduced phenomena promoted by nonlinear phononics are discussed in 'Revealing hidden phases and new states of matter'.

Metastable states. Impulsively induced electronic phases are typically short-lived, with lifetimes on the order of the electromagnetic pulse width or the energy relaxation time of the material. Yet, in quantum materials with corrugated free-energy landscapes, impulsive stimulation can trap the system in new phases at auxiliary free-energy minima, separated from the true ground states by a significant kinetic barrier[54–56]. These metastable phases persist indefinitely on experimental timescales but can be controllably erased by external parameters such as temperature and magnetic field.

Polaritons. These quasiparticles (Box 1, panel a) are hybrids of light and matter involving collective oscillations of charges in materials[25,57]. The most thoroughly investigated and utilized of these are surface plasmon-polaritons supported by electrons in conducting media and light. Other examples include phonon- and exciton-polaritons. A common denominator of many classes of polaritons is that they permit the confinement of light at the nanoscale, thereby dramatically enhancing light–matter interaction. Polaritons provide a natural route to strongly enhance the interaction of light and matter. As such, polaritons are well suited to increase rates of 'forbidden' transitions in solids[58], may enable efficient heat transfer at the nanoscale, and even alter chemical properties of molecules—a method dubbed polaritonic chemistry[59].

Direct hopping modulation and Floquet engineering. Time-periodic perturbation has recently emerged as a promising strategy for tuning the microscopic interaction parameters in a quantum many-body system. This dynamical approach, dubbed Floquet engineering, involves modulating the system at frequencies on par with or exceeding intrinsic interaction energy scales (Box 1, panel c). In the high-frequency regime, the system evolves under a simple effective equilibrium Hamiltonian with a hopping amplitude that is renormalized by a factor $J_0(\varepsilon)$, where J_0 is the zeroth Bessel function of the first kind, and ε is the aforementioned

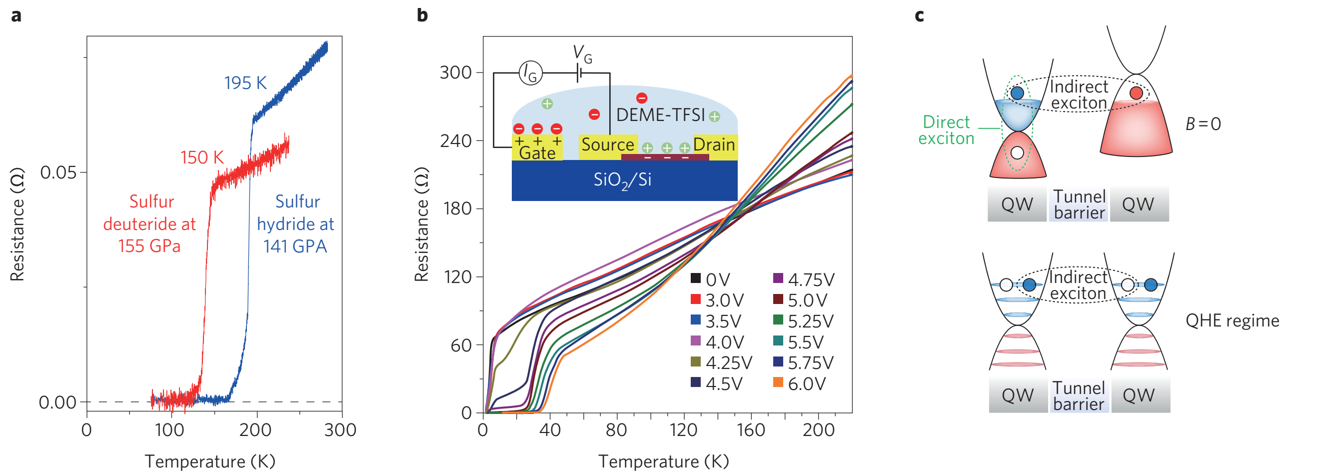

Figure 3 | Superconductivity and exciton condensates on demand. a, Resistance versus temperature traces for sulfur hydride (blue) and sulfur deuteride (red) revealing sharp superconducting transitions under pressure. **b**, Temperature dependence of the resistance for a FeSe microcrystal integrated in an electrical-double-layer transistor utilizing ionic liquid as the gate insulator. Data reveal tunable superconductivity with T_c controlled by the gate voltage. The thickness of the microcrystal is 10 nm. **c**, Optically excited particle–hole pairs combine to form short-lived, spatially direct excitons. Electron–hole pairing across a tunnel barrier prevents recombination, leading to long-lived, spatially indirect excitons. In the quantum Hall regime at large magnetic field, spatially indirect excitons can also result from coupling between partially filled Landau bands. Adapted from ref. 34, Macmillan Publishers Ltd (**a**); ref. 82, APS (**b**); and ref. 95, Macmillan Publishers Ltd (**c**).

Floquet parameter[60]. Therefore the hopping can in principle be tuned by the amplitude or frequency of the electromagnetic field (albeit in potential competition with effects that occur in the Keldysh tunnelling regime, $\gamma < 1$). In strongly correlated systems, magnetic exchange interactions, which are proportional to the hopping squared, also become highly tunable[60]. Floquet engineering has already been successfully implemented in ultracold atomic systems, where modulation is imparted by shaking the underlying optical lattice. However, implementation of Floquet engineering in solids, where modulation is imparted by external electromagnetic radiation, is still unrealized. A major challenge is that ultrashort laser pulses must be used to generate the requisite high driving amplitudes, which makes any Floquet phase short-lived and difficult to detect. In addition, questions about how to control the steady-state occupation of Floquet bands and to mitigate heating effects remain outstanding. However, recent advancements in ultrafast experimental techniques, theoretical simulations of time-domain experiments[61,62] and the development of driving protocols for population and thermal management[63,64] are boldly moving this field forward[65]. The recent successful imaging of a Floquet band structure (Fig. 1a) in Bi_2Se_3 (ref. 11), enabled by technological leaps in time-resolved angle-resolved photoemission spectroscopy (tr-ARPES)[66,67], is an exciting opening act to this grand pursuit.

Valley control and Berry phase modulation. The semiclassical dynamics of electrons in external fields are modified by the Berry curvature of Bloch states in momentum space, giving rise to an anomalous velocity that is responsible for phenomena such as the anomalous Hall effect[7]. Materials such as graphene and monolayer TMDs possess the electronic structure with two valleys, which contribute Berry curvatures of equal magnitude but opposite sign (Box 1, panel d). Through valley-selective resonant optical pumping or off-resonant electromagnetically induced a.c. Stark shifts[68], the net Berry curvature, and thus anomalous velocity related effects, can be controlled on demand. Another proposed route to manipulating Berry phase effects is via Floquet engineering of band structures[69], whereby electromagnetic driving is used to induce topologically trivial to non-trivial transitions in systems through dynamical breaking of time-reversal symmetry in systems like graphene[4,68] or through a reorganization of orbital textures in systems like spin–orbit coupled semiconductors[5,6].

Creating macroscopic quantum coherence

The condensation of bosons is arguably the most dramatic manifestation of a macroscopic quantum phenomenon in nature. In solids, superconductivity arising from Cooper pairing with long-range phase coherence is the archetype of quantum condensation. Indeed, the insights and advances in quantum matter arising from the study of superconductivity are unparalleled[14]. The notion of condensation extends beyond the domain of superconductivity to other bosonic excitations, including magnons, excitons and exciton-polaritons[70–72]. All these condensates are amenable to the full range of parameter manipulation in Fig. 2, allowing for the exploration of novel phases in a controlled fashion with the ultimate goal of 'condensation on demand'. Another goal is to enhance the maximum temperature at which a given condensate remains stable. We briefly consider some of the insightful advances in quantum condensates.

Superconductivity. Since the start of the new millennium the discovery of new superconductors includes MgB_2 (ref. 73), an entire class of materials in the Fe-based pnictides[74], and the realization of superconductivity above 200 K at high pressure in sulfur hydrides[34]. The latter exhibits a strong isotope effect in support of phonon mediated superconductivity (Fig. 3a and Box 1, panel b). Thus, pressure-induced superconductivity in sulfur compounds follows the phonon-centric paradigm at variance with Fe- and Cu-based high-T_c superconductors where magnetism is likely to play a prominent role in the pairing mechanism[75]. Mono- and few-layer FeSe is another recent surprise; reports of T_c for monolayer specimens on $SrTiO_3$ substrates range from 65–95 K, far in excess of the T_c~8 K of bulk FeSe[79]. The origin of this phenomenon is under debate with both interfacial doping and substrate-modified electron–phonon coupling implicated in the enhancement[80]. The transition temperature of few-layer FeSe can also be modified through electrostatic tuning[81,82] (Fig. 3b). Intriguingly, electric field-induced superconductivity, albeit at lower T_c, has also been observed in TMDs such as MoS_2 and 1T-$TiSe_2$ (refs 83,84) whereas cuprate high-T_c superconductors reveal a broadly tunable transition temperature[85]. Finally, we mention that non-equilibrium superconductivity is a rapidly

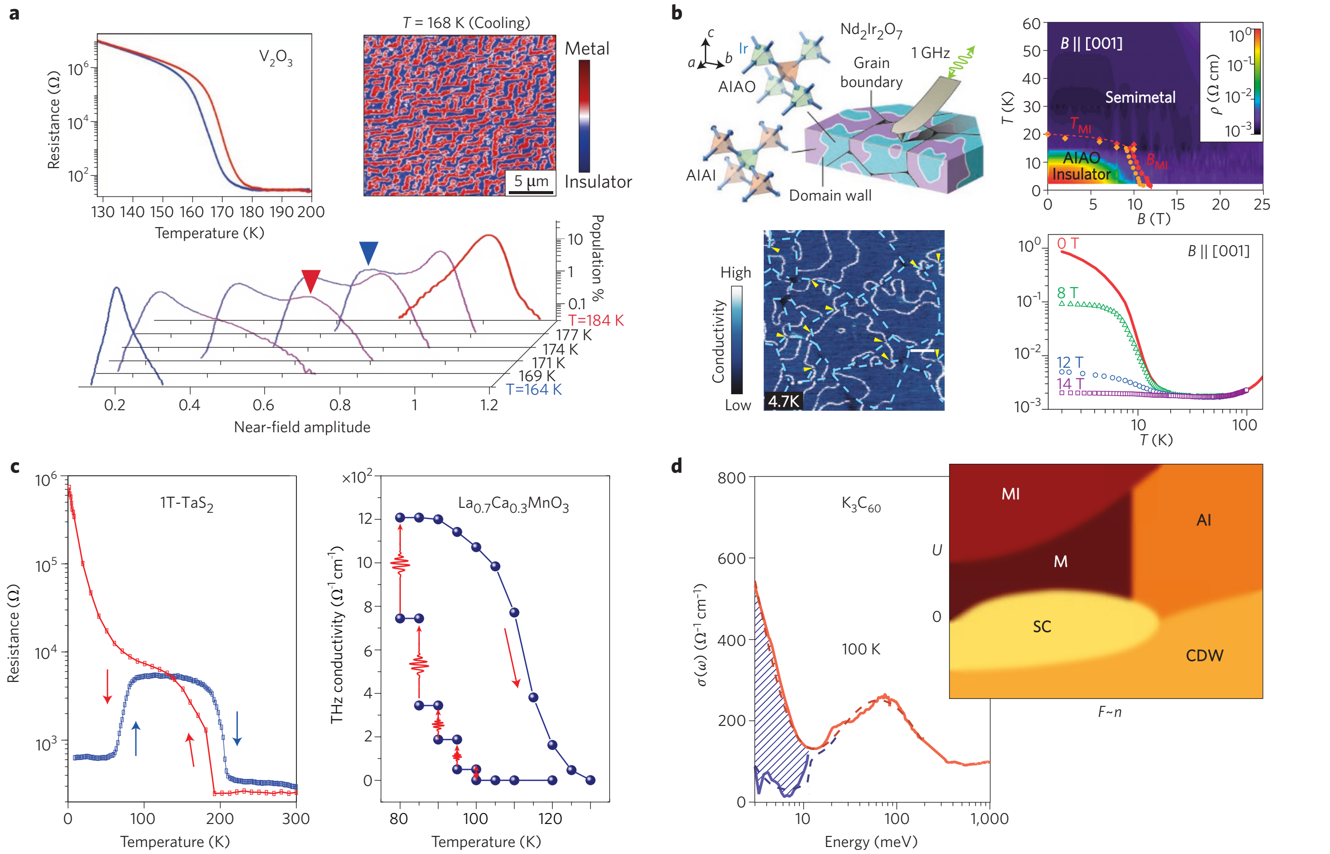

Figure 4 | Hidden and perturbation-enhanced phases of quantum materials. a, Nano-IR imaging of V_2O_3, revealing nanotexturing through the insulator-to-metal transition (IMT) with regions distinct from either insulating or metallic end phases. **b**, $Nd_2Ir_2O_7$ iridate with magnetic field controlled IMT, and conducting domain walls. **c**, Hidden metallic states in 1T-TaS_2 and strained $La_{0.7}Ca_{0.3}MnO_3$. In 1T-TaS_2, the low-temperature phase is insulating (red curve) becoming metallic upon photoexcitation (blue curve). Similarly, in strained $La_{0.7}Ca_{0.3}MnO_3$, the low-temperature phase is insulating, with a stepwise increase in the conductivity with photoexcitation and decreasing temperature. Subsequently, the original insulating state re-emerges with increasing temperature. **d**, Photoinduced superconducting-like gap in K_3C_{60} and calculations of the non-equilibrium phase diagram revealing strong dependence on average boson occupation. Adapted from ref. 101, Macmillan Publishers Ltd (**a**); ref. 102, AAAS (b); ref. 54, AAAS (**c**, left); ref. 56, Macmillan Publishers Ltd (**c**, right); ref. 103, Macmillan Publishers Ltd (**d**, left); and ref. 104, Macmillan Publishers Ltd (**d**, right).

developing research area (Fig. 4d), including the recent observation of the Higgs mode[86] in a disordered superconductor and in NbN using time-resolved terarhertz spectroscopy[87].

Magnon condensates. These condensates constitute a well-established topic, building on the detailed correspondence between quantum spins and Bose–Einstein condensates (BEC)[88,89]. Magnon condensates include those that are thermodynamically accessible and those created through non-equilibrium excitation. Examples of the former are realized with an applied magnetic field, which tunes the magnon density to access the dilute limit BEC (analogous to chemical potential tuning in atomic condensates). Pioneering results include demonstrations of condensation of antiferromagnetic dimers in $TlCuCl_3$ (ref. 70) and $BaCuSi_2O_6$ (ref. 90). Recent work focused on elucidating a quantum critical point in $BaCuSi_2O_6$ (ref. 91) and spontaneous electric polarization in $TlCuCl_3$ on entering the magnon condensate phase[92]. These results suggest the possibility of condensate control with an applied electric field. Non-equilibrium magnon condensates can be generated with microwave pulses to control the chemical potential independent of temperature. At a critical pumping power, a sufficient magnon density is created that can subsequently thermalize and condense. This was first observed using light-scattering spectroscopy in thin films of yttrium iron garnet[93] (YIG), a ferrimagnet that can be efficiently pumped and has a long spin–lattice relaxation time, allowing for magnon condensation at ambient temperature. More recently, experiments on YIG films uncovered a room-temperature magnon supercurrent[94]: a macroscopic collective motion of magnon condensate subjected to a thermal gradient. This result is appealing in the context of spintronic devices operational at ambient temperature.

Exciton and exciton-polariton condensates. Indirect exciton and exciton-polariton condensates, created through optical excitation, represent the state-of-the-art with respect to on-demand control of macroscopic coherent states of matter. Coupled layers of two-dimensional electron gas (2DEG) in GaAs quantum wells remain the gold standard in the study of these condensates[71,96]. Van der Waals materials such as graphene and TMDs also offer considerable promise in creating designer condensates. Layer-by-layer tuning of the 2DEG interlayer spacing (and therefore coupling) is possible using insulating spacers of hexagonal boron nitride (hBN). This convenient tuning knob complements gating control of the intralayer doping. A confluence of light effective masses, high exciton binding energies (0.4–0.9 eV) and prominence of many-body effects in TMD-based heterostructures holds promise for the realization of excitonic condensates and superfluids under ambient conditions[97,98]. Data for two bilayer graphene specimens separated by a thin spacer of hBN in the quantum Hall regime offer the enticing hints of exciton condensation[95]. Indirect excitons in this system do not require optical

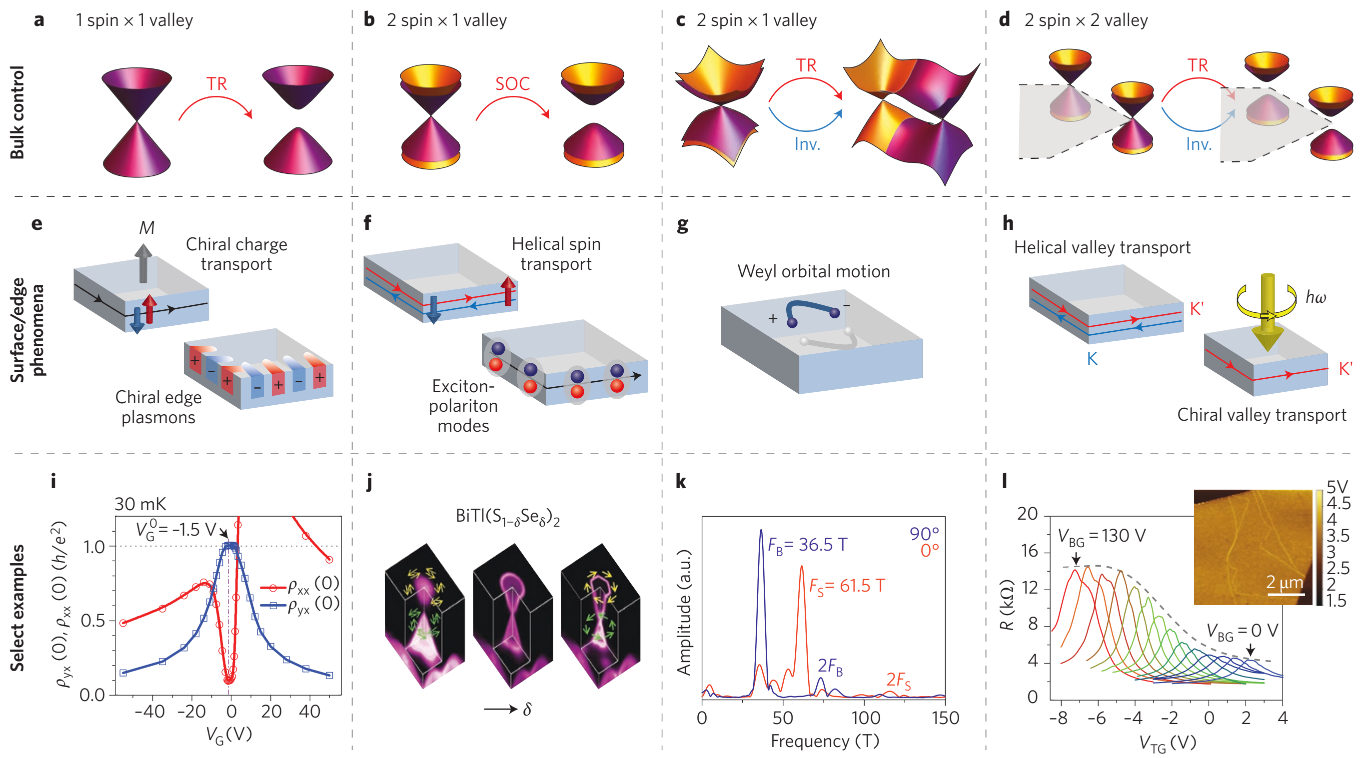

Figure 5 | Topological properties on demand. a–d, Schematic of mechanisms for tuning between trivial (left) and topological (right) bulk band structures, either by breaking time-reversal symmetry (TR), breaking inversion symmetry (Inv.) or increasing spin–orbit coupling (SOC). **e–h**, Examples of edge/surface states that emerge upon undergoing the above bulk topological transitions. **i–l**, Select experimental demonstrations of the topological phase transitions via edge/surface sensitive measurements: (**i**) evidence of a magnetization controlled quantum anomalous Hall phase via quantized edge transport; (**j**) evidence of a chemical substitution controlled trivial to 3D topological insulator via surface state dispersion; (**k**) evidence of an inversion symmetry breaking induced Weyl semimetal phase via exotic bulk-to-surface quantum oscillations; (**l**) evidence of a quantum valley Hall phase via quantized transport of domain wall edge states. Adapted from ref. 135, AAAS (**i**); ref. 138, AAAS (**j**); ref. 139, Macmillan Publishers Ltd (**k**); and ref. 136 Macmillan Publishers Ltd (**l**).

excitation, forming instead between partially filled Landau levels (Fig. 3c). Microcavity exciton-polariton condensates continue to produce exciting results[72]. Creating a thermalized condensate has proved challenging since the thermal equilibration time is typically longer that the polariton lifetime. Yet, the thermalized limit can be achieved through the design of higher-Q microcavities[99]. We conclude this section mentioning an interesting theoretical prediction—namely, an exciton-polariton condensate in proximity to a 2DEG is expected to promote superconducting pairing[100]. The unmatched degree of controls attainable in vdW heterostructures may enable the experimental validation of this exciting proposal.

Revealing hidden phases and new states of matter

Insulator-to-metal transitions (IMT) are a hallmark of many families of quantum materials. It is now feasible to investigate these transitions in the regimes of ultrahigh electric/magnetic fields, and ultrafast and intense optical pulses in concert with nanoscale spatial resolution. These previously unattainable means of control and inquiry have uncovered a host of metastable states and 'hidden' phases not apparent in common phase diagrams of quantum materials that are typically measured at (or near) equilibrium using area-averaging probes.

Anomalous metallicity at the nanoscale. We begin with the veteran quantum material V_2O_3, often referred to as a prototypical Mott insulator. Yet, this compound continues to uncover novel facets of correlations. The electronic transition at T_{IMT}~160 K is accompanied by a structural transformation. Furthermore, the low-T insulator is antiferromagnetically ordered in accord with the expectations of Mott theory. The physics of the first-order phase transition is apparent in the nano-infrared image in Fig. 4a. The scattering amplitude results shown in the image and in the histogram plot in the lower panel can be interpreted in terms of the local conductivity[101]. These data reveal coexisting metallic (red) and insulating (blue) domains. All these attributes are generic to other correlated oxides undergoing the IMT. An unexpected result is the continuous evolution of the local infrared conductivity in V_2O_3 across the IMT. This finding is at variance with the conventional picture of a first-order transition where the metallic volume fraction increases with temperature at the expense of the insulating volume fraction, with the two phases remaining electronically unchanged throughout the transition. The observed continuous character of the IMT was predicted within a model allowing for a long-range interaction between the domains[105], but remained elusive since the observation required a scanning probe experiment with nanoscale resolution.

Correlated oxides with strong spin–orbit interaction. A family of pyrochlore $R_2Ir_2O_7$ materials (where R stands for rare earth elements) and $Cd_2Os_2O_7$ compounds exhibit magnetic ordering of the Ir (Os) 5d moments with an all-in all-out (AIAO)-type structure[106]. The AIAO magnetic structure implies that all magnetic moments on one tetrahedron point either inwards (all-in) or outwards (all-out) from its centre (Fig. 4b). The domain walls between two distinct types of AIAO domain are believed to play a profound role both in transport and electrodynamics of Ir- and Os-based systems. Specifically, the boundaries between two inequivalent domains were predicted to host metallic states[107] at $T<T_{IMT}$. These domain walls were visualized in AIAO compound $Nd_2Ir_2O_7$ using a scanning microwave probe[102]

that is sensitive to the local conductivity. Notably, the density of the domain walls in $Nd_2Ir_2O_7$ can be tuned with an applied magnetic field: a remarkable effect that accounts for anomalies detected in area-averaged transport studies. The nature of the electronic state of these conducting domain walls remains unexplored; future experiments are needed to verify the prediction of Weyl states associated with the domain walls[108].

Metallicity under static *E* or *B* fields. The discovery of a static magnetic field-tuned IMT in $Nd_2Ir_2O_7$ is an elegant demonstration of how dramatic electronic reconstruction can be imparted by moderate field strengths (~10 T). The confluence of strong spin–orbit coupling, Coulomb repulsion and geometrical frustration in $Nd_2Ir_2O_7$ marginally stabilizes a magnetically ordered insulating ground state that is on the precipice of a metallic transition. Interestingly, the insulating state is endowed with both Mott and Slater characteristics, namely a large insulating gap of around 45 meV (~800 T) that is linked to a $Q = 0$ magnetic order. Therefore, application of a magnetic field at the Zeeman energy scale, far below the gap energy scale, is sufficient to drive a drop in resistivity by three orders of magnitude. Analogous phenomena can also be triggered using static electric fields. The Mott gap in the multi-orbital Mott insulator Ca_2RuO_4, for example, has been reported to collapse under application of a weak electric field (~40 V cm^{-1})[109] far below the energy gap scale. While the exact mechanism is still unsettled, it seems likely that novel phenomena such as a many-body Zener effect and orbital depolarization are at play.

Metastable states. Stimulation with ultrashort optical pulses has been utilized to induce phase transitions in a host of quantum materials via photothermal quenches, field-induced tunnelling and phonon excitation, among others[2,110–113]. In some materials, the transition between two thermally accessible phases proceeds through a distinct transient phase. VO_2 is an interesting example, with evidence of a short-lived monoclinic metallic phase[114] that is electronically distinct from the high-temperature metal phase with a rutile crystal structure. Nonetheless, in nearly all cases to date, these induced phases are ephemeral with lifetimes ranging from picoseconds to nanoseconds. Impulsive photoexcitation can also generate metastable quantum phases in correlated electron systems, separated from the true ground state by a kinetic barrier. These phases persist indefinitely on timescales of days and can be erased by tuning external parameters such as temperature or magnetic field. Photoinduced metastable IMTs have been observed in the CDW material 1T-TaS_2 (refs 54,115) and in the strained manganite $La_{0.7}Ca_{0.3}MnO_3$ (LCMO; ref. 56), with the results highlighted in Fig. 4c[55]. In TaS_2, 1.55-eV photoexcitation at low temperatures in the commensurate CDW phase results in a decrease in the resistance by three orders of magnitude arising from collective polaron reordering[54]. Similarly, at low temperatures, strained LCMO is a charge-ordered antiferromagnetic insulator where 1.55-eV excitation results in a collapse to a ferromagnetic metallic state, with strong magneto-elastic coupling being of importance[56]. In both cases, a minimum fluence (~1 mJ cm^{-2}) is required to achieve metastability suggestive of the need for a critical photoexcited volume to prevent collapse back to the initial phase. LCMO and 1T-TaS_2 are drastically different in terms of their electronic structure and crystallography; yet they exhibit certain similarities of photoinduced metastability. This indicates the need for further studies to understand the conditions and processes that result in photoinduced metastability, and to search for other materials that can exhibit robust metastability.

Phononic controls of quantum materials. A prominent early example is light-induced metallicity of the correlated oxide $Pr_{0.7}Ca_{0.03}MnO_3$ prompted by a collapse of the bandgap via coherent excitation of Mn–O vibrational modes[112]. Resonant phonon excitation minimizes both electron and lattice heating: two detrimental effects that are difficult to avoid under non-discriminative pumping of materials with convenient near-IR or visible lasers. Apart from inducing metallicity, phononic excitation has been employed to melt orbital order[116] and trigger strong effective magnetic fields[117]. A particularly intriguing series of experiments has reported on phononically driven enhancement of superconducting correlations both in the cuprates and in K_3C_{60} (refs 103,118). Figure 4d shows the real part of the optical conductivity for K_3C_{60} at 100 K, well above the bulk T_c of this compound. At equilibrium (red curve) a Drude-like response is observed. On excitation with 0.18-eV pulses (blue curve), a gap appears that is reminiscent of superconductivity[103]. These experiments have motivated theoretical work, both to understand the nature of lattice dynamics arising from nonlinear phonon excitation, and to elucidate the possible origin of the superconducting enhancement[118,119]. The inset of Fig. 4d displays a theoretical phase diagram in terms of the on-site Coulomb potential U and the average boson occupation, predicting enhanced superconductivity along with other phases (for example, an Anderson insulating phase that does not exist in equilibrium)[104].

Need for attosecond transients. A fundamental problem in ultrafast experiments is the need to disentangle the electronic and lattice contributions in the course of light-activated processes. Naturally, the electronic processes are much faster than dynamics involving the lattice, which are difficult to probe using standard lasers with pulses limited to tens of femtoseconds. For that reason, the light-induced collapse of the band gap in VO_2 observed in ref. 120 was referred to as an 'instantaneous' process. We note that attosecond pump–probe experiments are becoming increasingly adept at distinguishing these seemingly instantaneous electronic phenomena from slower femtosecond processes involving the lattice[121]. Hence, a broader application of attosecond methodology to quantum materials is poised to produce significant advances. An added value of this line of research is that attosecond pulses also enable damage-free exposure of insulating solids to electric fields of the order of the Zener critical field $F_{crit} = E_g/ea$. Ultra-rapid reversible optical waveforms were shown to increase the a.c. conductivity of wide-bandgap dielectrics by more than 18 orders of magnitude within 1 femtosecond[13,122]. These experiments open pathways for signal processing in the petahertz domain, which is not attainable with common electronics.

Topological phenomena under control

Within the Landau paradigm, phases of matter are distinguished by their symmetries. However, there exists a finer level of classification based not on symmetry, but rather on the topological or entanglement properties of the electronic wavefunction. The latter give rise to exotic phases of matter with protected states and anomalous static and finite-frequency response functions that stem from geometric (Berry) phase effects[26,123–126]. In this section, we focus on strategies to realize topological phenomena on demand by manipulating Berry phases associated with linear or quadratic band crossings of the bulk electronic structure (Fig. 5). We will not discuss interacting topological phases such as topological superconductors—a burgeoning area of research with potential applications to quantum computing—because a number of excellent reviews already exist[127,128].

Topological insulators. This class of materials can be born from trivial insulators by closing the gap in the bulk Dirac spectrum and reopening it with inverted orbital character (Fig. 5b). This type of trivial-to-topological insulator transition can be achieved via impurity doping, pressure/strain, temperature, heterostructuring/electrostatic-gating, or even optical stimulation, delivering helical edge/surface states with non-trivial Berry phase on demand[4–6,126,129–133].

Quantum anomalous Hall (Chern) insulators. By opening a gap in the 2D surface Dirac spectrum of a 3D topological insulator through spontaneous time-reversal symmetry breaking and tuning the Fermi level to lie inside the surface gap[134], one is able to produce a quantum anomalous Hall insulator. This non-trivial phase exhibits a quantized Hall conductance e^2/h analogous to conventional quantum Hall insulators, but does not require any externally applied magnetic field. It has been experimentally shown that a quantum anomalous Hall phase[135] arises in gated ferromagnetic three-dimensional topological insulator $Cr_y(Bi_xSb_{1-x})_{2-y}Te_3$ devices below a Curie temperature T_C = 15 K where the chiral modes can be switched on and off by varying the temperature across T_C.

Quantum valley Hall insulators. These materials are gapped one-dimensional systems that host counter-propagating one-dimensional chiral edges states with opposite valley index. In the absence of valley-mixing processes, these edge states are effectively topologically protected and can be regarded as the valley analogue of a two-dimensional topological insulator (Fig. 5d). These conditions have recently been experimentally realized at the domain walls between AB and BA stacked bilayer graphene in the presence of an externally applied electric field[136], which lifts the degeneracy of its quadratic band touching points. By switching the electric field, and in turn the bandgap, on and off, chiral valley polarized edge states can be created and destroyed controllably. It has been theoretically proposed that an even more exotic insulating phase with a single chiral edge state can be realized by driving such systems with circularly polarized light[137], which breaks the valley degeneracy. This would offer a remarkable capability to control both the valley index and direction of current via the photon helicity.

Weyl semimetals. These three-dimensional topological phases of matter, unlike all previously mentioned examples in Fig. 5, are gapless. They can be realized by splitting a lattice symmetry-protected doubly spin degenerate bulk Dirac cone (Dirac semimetal) into two singly degenerate Weyl cones either by breaking lattice inversion symmetry or time-reversal symmetry[124] (Fig. 5c). Weyl points are protected by a topological chiral charge and are connected to one another via open arc-like surface states, forming an unusual conducting pathway (Weyl orbit) between the top and bottom surfaces through the bulk. Recently, spectroscopic evidence of surface Fermi arcs[124] and magneto-transport evidence of chiral anomalous transport and closed Weyl orbits[139] have confirmed the existence of inversion symmetry broken families of Weyl semimetals. On-going efforts to realize their time-reversal broken counterparts via Zeeman splitting[140], spontaneous magnetization[141–144] or even circularly polarized light[145] may ultimately enable on-demand switching of the Weyl phase by temperature, magnetic field or optical irradiation, and potentially allow controllable positioning of Weyl points in momentum space.

Floquet topological states. Floquet engineering has recently been successfully applied in ultracold atomic systems to create synthetic gauge fields for stabilizing topological band structures in optical lattices[78]. Although this strategy has yet to be experimentally demonstrated in condensed-matter systems, theoretical progress is being made at a rapid pace. Dynamical engineering protocols for manipulating Berry curvatures in Dirac systems[146], transforming trivial materials into Floquet topological insulators[5,6,130], *p*-wave superconductors[147], Weyl semimetals[145,148], chiral spin liquids[149] and quantum Hall phases without external magnetic fields[4,68,149], eagerly await experimental implementation. These endeavours will draw heavily from knowledge accumulated in the cold-atom and molecule community and forge greater synergy with condensed-matter physics.

Topological plasmons and polaritons. Recently, the aforementioned strategies for creating topologically protected electronic edge/surface states have been extended to other types of excitations. For example, chiral plasmons—one-way-propagating collective oscillations of the itinerant electron sea—have been proposed to occur at the edges of anomalous Hall metals and other multivalley conducting media where both time-reversal and inversion symmetries are broken[27,150]. Plasmon-polariton chirality is a direct consequence of non-vanishing Berry curvature in a medium that can be induced on demand by driving, for example, valley degenerate semiconductors with circularly polarized light. Topological exciton-polaritons have also been proposed in monolayer TMDs subject to a finite magnetic field or circularly polarized optical stimulation[151]. Topological polaritons can be turned off simply by switching off the magnetic field or light, or have their propagation reversed by flipping the sign of the magnetic field or light helicity.

Looking into the future

On-demand control of quantum materials is emerging as a vibrant area of research offering unprecedented access to new physics. In this Review, we described some of the efforts to attain novel phases in quantum materials utilizing perturbation protocols in Fig. 2.

At present, state-of-the-art ultrafast methods offer a near-complete characterization of the transient state[152]. Indeed, tr-ARPES provides a direct probe of the transient electronic structure[66,67,120,153], tabletop and accelerator-based X-ray free-electron lasers readily capture momentary crystal arrangements[118,154], nonlinear optical methods can directly interrogate the symmetries of quantum phases and their host lattices[30,155–158], while optical and soft X-ray techniques document electronic excitations, in some cases with elemental and orbital specificity[159]. Importantly, mesoscopic phenomena that are prevalent in quantum materials lead to new time and energy scales, as documented in various ultrafast studies[110,160]. Modern scanning optical probe tools are set to dramatically advance our understanding of mesoscopic dynamics, visualizing local transient phenomena at nano- and mesoscales[161–163]. A future challenge is to create ground-state or continuous-wave-driven steady-state versions of enigmatic nano- and mesoscale phenomena currently attainable only in transient regimes. An appealing proposition is to exploit a combination of materials synthesis and heterostructuring to engineer free-energy landscapes in order to replicate transient properties. If successful, this approach will augment a largely serendipitous approach to materials discovery with predictive and targeted searches for new systems with desired properties.

Nonlinear phenomena in quantum materials present enticing possibilities with as yet untapped potential for properties control. Impulsive optical generation of coherent charge, spin or lattice normal modes in solids is rapidly advancing. New experiments are beginning to explore the possibility of coherently amplifying these modes and to dynamically stabilize new electronic phases. A recent success is parametric amplification of Josephson plasma waves in a cuprate superconductor using strong THz fields[46]. This approach exploits the highly nonlinear response of the plasma to the THz electric field. Other sophisticated driving protocols involving simultaneous excitation of more than one lattice mode with controlled relative phases[117], pulse shaping[164], multipulse excitation[165] or simultaneous multicolour optical excitation[166] may allow dynamical stabilization of various phases, including Hall and topological states. Multidimensional optical spectroscopies remain under-exploited in these tasks despite the unmatched ability of these methods to go beyond ensemble-averaged properties and their potential to 'see through' inhomogeneous broadening of resonance lines[167]. Finally, the ability to measure electric-field vacuum fluctuations in the time domain may provide new routes to measure and control quantum phenomena in materials[168].

In tandem with improvements in experimental detection capabilities, theoretical predictions of new forms and phases of quantum matter are becoming increasingly precise[6,53,69,104,129,130,151,169,170]. Theory is indispensable for devising driving protocols to realize new quantum phases on demand, beyond the parameter regimes of existing materials. These include long-sought symmetry-broken phases such as room-temperature superconductors, and new topological phases featuring exotic quasiparticles[26,124–127,171,172] that lie beyond the realm of elementary particle physics. Theory is poised to guide the search and classification of new phases that are fundamentally non-equilibrium, with the recently discovered discrete time crystal being a prime example[173,174]. With these concerted theoretical and experimental efforts, the quantum materials community is on track to fully unlock a world of possibilities of on-demand control.

Received 12 May 2017; accepted 22 September 2017; published online 25 October 2017

References

1. Subatomic opportunities: Quantum leaps. *The Economist* (11 March 2017).
2. Zhang, J. & Averitt, R. D. Dynamics and control in complex transition metal oxides. *Annu. Rev. Mater. Res.* **44,** 19–43 (2014).
3. Basov, D. N., Averitt, R. D., van der Marel, D., Dressel, M. & Haule, K. Electrodynamics of correlated electron materials. *Rev. Mod. Phys.* **83,** 471–541 (2011).
4. Oka, T. & Aoki, H. Photovoltaic Hall effect in graphene. *Phys. Rev. B* **79,** 81406 (2009).
5. Inoue, J. & Tanaka, A. Photoinduced transition between conventional and topological insulators in two-dimensional electronic systems. *Phys. Rev. Lett.* **105,** 017401 (2010).
6. Lindner, N. H., Refael, G. & Galitski, V. Floquet topological insulator in semiconductor quantum wells. *Nat. Phys.* **7,** 490–495 (2011).
This theoretical paper proposed a method to produce a topologically non-trivial electronic state via photoexcitation of semiconductor.
7. Xiao, D., Chang, M.-C. & Niu, Q. Berry phase effects on electronic properties. *Rev. Mod. Phys.* **82,** 1959–2007 (2010).
8. Nagaosa, N., Sinova, J., Onoda, S., MacDonald, A. H. & Ong, N. P. Anomalous Hall effect. *Rev. Mod. Phys.* **82,** 1539–1592 (2010).
9. Morimoto, T., Zhong, S., Orenstein, J. & Moore, J. E. Semiclassical theory of nonlinear magneto-optical responses with applications to topological Dirac/Weyl semimetals. *Phys. Rev. B* **94,** 245121 (2016).
10. Mahmood, F. *et al.* Selective scattering between Floquet–Bloch and Volkov states in a topological insulator. *Nat. Phys.* **12,** 306–310 (2016).
11. Wang, Y. H., Steinberg, H., Jarillo-Herrero, P. & Gedik, N. Observation of Floquet–Bloch states on the surface of a topological insulator. *Science* **342,** 453–457 (2013).
12. Badoux, S. *et al.* Change of carrier density at the pseudogap critical point of a cuprate superconductor. *Nature* **531,** 210–214 (2016).
13. Schiffrin, A. *et al.* Optical-field-induced current in dielectrics. *Nature* **493,** 70–74 (2013).
14. Keimer, B., Kivelson, S. A., Norman, M. R., Uchida, S. & Zaanen, J. From quantum matter to high-temperature superconductivity in copper oxides. *Nature* **518,** 179–186 (2015).
15. Taillefer, L. Superconductivity and quantum criticality. *Phys. Canada* **67,** 109–112 (2011).
16. Sebastian, S. E., Harrison, N. & Lonzarich, G. G. Towards resolution of the Fermi surface in underdoped high-T_c superconductors. *Rep. Prog. Phys.* **75,** 102501 (2012).
17. Zhou, Y. & Ramanathan, S. Correlated electron materials and field effect transistors for logic: a review. *Crit. Rev. Solid State Mater. Sci.* **38,** 286–317 (2013).
18. Inoue, I. H. & Rozenberg, M. J. Taming the Mott transition for a novel Mott transistor. *Adv. Funct. Mater.* **18,** 2289–2292 (2008).
19. Strukov, D. B., Snider, G. S., Stewart, D. R. & Williams, R. S. The missing memristor found. *Nature* **453,** 80–83 (2008).
20. Driscoll, T. *et al.* Memristive adaptive filters. *Appl. Phys. Lett.* **97,** 093502 (2010).
21. Martin, I., Blanter, Ya. M. & Morpurgo, A. F. Topological confinement in bilayer graphene. *Phys. Rev. Lett.* **100,** 036804 (2008).
22. Ye, Z., Sun, D. & Heinz, T. F. Optical manipulation of valley pseudospin. *Nat. Phys.* **13,** 26–29 (2016).
23. Lumer, Y., Plotnik, Y., Rechtsman, M. C. & Segev, M. Self-localized states in photonic topological insulators. *Phys. Rev. Lett.* **111,** 243905 (2013).
24. Lu, L., Joannopoulos, J. D. & Soljačić, M. Topological photonics. *Nat. Photon.* **8,** 821–829 (2014).
25. Low, T. *et al.* Polaritons in layered 2D materials. *Nat. Mater.* **16,** 182–194 (2016).
26. Qi, X.-L. & Zhang, S.-C. Topological insulators and superconductors. *Rev. Mod. Phys.* **83,** 1057–1110 (2011).
27. Song, J. C. W. & Rudner, M. S. Chiral plasmons without magnetic field. *Proc. Natl Acad. Sci. USA* **113,** 4658–4663 (2016).
28. Morimoto, T. & Nagaosa, N. Topological nature of nonlinear optical effects in solids. *Sci. Adv.* **2**, e1501524 (2016).
29. Cook, A. M., Fregoso, B. M., De Juan, F., Coh, S. & Moore, J. E. Design principles for shift current photovoltaics. *Nat. Commun.* **8,** 14176 (2017).
30. Wu, L. *et al.* Giant anisotropic nonlinear optical response in transition metal monopnictide Weyl semimetals. *Nat. Phys.* **13,** 350–355 (2017).
31. Ma, Q. *et al.* Direct optical detection of Weyl fermion chirality in a topological semimetal. *Nat. Phys.* **13,** 842–847 (2017).
32. Wu, S. *et al.* Monolayer semiconductor nanocavity lasers with ultralow thresholds. *Nature* **520,** 69–72 (2015).
33. Tokura, Y., Kawasaki, M. & Nagaosa, N. Emergent functions of quantum materials. *Nat. Phys.* http://doi.org/10.1038/nphys4274 (2017).
34. Drozdov, A. P., Eremets, M. I., Troyan, I. A., Ksenofontov, V. & Shylin, S. I. Conventional superconductivity at 203 kelvin at high pressures in the sulfur hydride system. *Nature* **525,** 73–76 (2015).
35. Zhong, D. *et al.* Van der Waals engineering of ferromagnetic semiconductor heterostructures for spin and valleytronics. *Sci. Adv.* **3**, e1603113 (2017).
36. Efetov, D. K. *et al.* Specular interband Andreev reflections at van der Waals interfaces between graphene and $NbSe_2$. *Nat. Phys.* **12,** 328–332 (2016).
37. Levy, N. *et al.* Strain-induced pseudo-magnetic fields greater than 300 tesla in graphene nanobubbles. *Science* **329,** 544–547 (2010).
38. Novoselov, K. S., Mishchenko, A., Carvalho, A. & Castro Neto, A. H. 2D materials and van der Waals heterostructures. *Science* **353,** aac9439 (2016).
39. Kumar, R. K. *et al.* Super-ballistic flow of viscous electron fluid through graphene constrictions. *Nat. Phys.* http://doi.org/10.1038/nphys4240 (2017).
40. Chakhalian, J., Freeland, J. W., Millis, A. J., Panagopoulos, C. & Rondinelli, J. M. Colloquium: Emergent properties in plane view: Strong correlations at oxide interfaces. *Rev. Mod. Phys.* **86,** 1189–1202 (2014).
41. Kim, T. H. *et al.* Polar metals by geometric design. *Nature* **533,** 68–72 (2016).
42. Gerber, S. *et al.* Three-dimensional charge density wave order in $YBa_2Cu_3O_{6.67}$ at high magnetic fields. *Science* **350,** 949–952 (2015).
43. Chan, M. K. *et al.* Single reconstructed Fermi surface pocket in an underdoped single-layer cuprate superconductor. *Nat. Commun.* **7,** 12244 (2016).
44. Kampfrath, T., Tanaka, K. & Nelson, K. A. Resonant and nonresonant control over matter and light by intense terahertz transients. *Nat. Photon.* **7,** 680–690 (2013).
45. Liu, M. *et al.* Terahertz-field-induced insulator-to-metal transition in vanadium dioxide metamaterial. *Nature* **487,** 345–348 (2012).
46. Rajasekaran, S. *et al.* Parametric amplification of a superconducting plasma wave. *Nat. Phys.* **12,** 1012–1016 (2016).
47. Steinleitner, P. *et al.* Direct observation of ultrafast exciton formation in a monolayer of WSe_2. *Nano Lett.* **17,** 1455–1460 (2017).
48. Oka, T. Nonlinear doublon production in a Mott insulator: Landau–Dykhne method applied to an integrable model. *Phys. Rev. B.* **86,** 075148 (2012).
49. Mayer, B. *et al.* Tunneling breakdown of a strongly correlated insulating state in VO_2 induced by intense multiterahertz excitation. *Phys. Rev. B* **91,** 235113 (2015).
50. Kirilyuk, A., Kimel, A. V & Rasing, T. Ultrafast optical manipulation of magnetic order. *Rev. Mod. Phys.* **82,** 2731–2784 (2010).
51. Matsukura, F., Tokura, Y. & Ohno, H. Control of magnetism by electric fields. *Nat. Nanotech.* **10,** 209–220 (2015).
52. Först, M. *et al.* Nonlinear phononics as an ultrafast route to lattice control. *Nat. Phys.* **7,** 854–856 (2011).
53. Subedi, A., Cavalleri, A. & Georges, A. Theory of nonlinear phononics for coherent light control of solids. *Phys. Rev. B* **89,** 220301 (2014).
54. Stojchevska, L. *et al.* Ultrafast switching to a stable hidden quantum state in an electronic crystal. *Science* **344,** 177–180 (2014).
55. Kiryukhin, V. *et al.* An X-ray-induced insulator–metal transition in a magnetoresistive manganite. *Nature* **386,** 813–815 (1997).
Discovery of persistent metallic state in manganites induced by illumination with X-rays.
56. Jingdi Zhang et. al. *et al.* Cooperative photoinduced metastable phase control in strained manganite films. *Nat. Mater.* **15,** 956–960 (2016).
57. Basov, D. N., Fogler, M. M. & García de Abajo, F. J. Polaritons in van der Waals materials. *Science* **354**, aag1992 (2016).
58. Rivera, N., Kaminer, I., Zhen, B., Joannopoulos, J. D. & Soljačić, M. Shrinking light to allow forbidden transitions on the atomic scale. *Science* **353,** 263–269 (2016).
59. Flick, J. *et al.* Atoms and molecules in cavities, from weak to strong coupling in quantum-electrodynamics (QED) chemistry. *Proc. Natl Acad. Sci. USA* **12,** 3026–3034 (2017).
60. Mentink, J. H., Balzer, K. & Eckstein, M. Ultrafast and reversible control of the exchange interaction in Mott insulators. *Nat. Commun.* **6,** 6708 (2015).
61. Wang, Y., Claassen, M., Moritz, B. & Devereaux, T. P. Producing coherent excitations in pumped Mott antiferromagnetic insulators. Preprint at http://arxiv.org/abs/1706.06228v1 (2017).
62. Dehghani, H. & Mitra, A. Optical Hall conductivity of a Floquet topological insulator. *Phys. Rev. B* **92,** 165111 (2015).
63. Iadecola, T., Neupert, T. & Chamon, C. Occupation of topological Floquet bands in open systems. *Phys. Rev. B* **91,** 235133 (2015).

64. Seetharam, K. I., Bardyn, C.-E., Lindner, N. H., Rudner, M. S. & Refael, G. Controlled population of Floquet–Bloch states via coupling to Bose and Fermi baths. *Phys. Rev. X* **5**, 041050 (2015).
65. De Giovannini, U., Hübener, H. & Rubio, A. Monitoring electron–photon dressing in WSe_2. *Nano Lett.* **16,** 7993–7998 (2016).
This article offers the most detailed description the formation of quasistatic electronic structure under periodic electromagnetic excitation.
66. Schmitt, F. *et al.* Transient electronic structure and melting of a charge density wave in $TbTe_3$. *Science* **321,** 1649–1652 (2008).
67. Gerber, S. *et al.* Femtosecond electron-phonon lock-in by photoemission and x-ray free-electron laser. *Science* **357,** 71–75 (2017).
The authors succeeded to synchronize for the first time transient photoemission and transient X-ray studies by locking into a coherent phonon mode.
68. Xu, X., Yao, W., Xiao, D. & Heinz, T. F. Spin and pseudospins in layered transition metal dichalcogenides. *Nat. Phys.* **10,** 343–350 (2014).
Excellent review article discussing valley control of electronic and optical phenomena in TMD compounds.
69. Eckardt, A. & Anisimovas, E. High-frequency approximation for periodically driven quantum systems from a Floquet-space perspective. *New J. Phys.* **17,** 093039 (2015).
70. Rüegg, C. *et al.* Bose–Einstein condensation of the triplet states in the magnetic insulator $TlCuCl_3$. *Nature* **423,** 62–65 (2003).
71. Eisenstein, J. P. & Macdonald, A. H. Bose–Einstein condensation of excitons in bilayer electron systems. *Nature* **432,** 691–694 (2004).
72. Byrnes, T., Kim, N. Y. & Yamamoto, Y. Exciton–polariton condensates. *Nat. Phys.* **10,** 803–813 (2014).
73. Nagamatsu, J., Nakagawa, N., Muranaka, T., Zenitani, Y. & Akimitsu, J. Superconductivity at 39 K in magnesium diboride. *Nature* **410,** 63–64 (2001).
74. Johnston, D. C. The puzzle of high temperature superconductivity in layered iron pnictides and chalcogenides. *Adv. Phys.* **59,** 803–1061 (2010).
75. Basov, D. N. & Chubukov, A. V. Manifesto for a higher T_c. *Nat. Phys.* **7,** 272–276 (2011).
76. Graf, J. *et al.* Nodal quasiparticle meltdown in ultrahigh-resolution pump-probe angle-resolved photoemission. *Nat. Phys.* **7,** 805–809 (2011).
77. Cilento, F. *et al.* In search for the pairing glue in cuprates by non-equilibrium optical spectroscopy. *J. Phys. Conf. Ser.* **449,** 012003 (2013).
78. Goldman, N., Budich, J. C. & Zoller, P. Topological quantum matter with ultracold gases in optical lattices. *Nat. Phys.* **12,** 639–645 (2016).
79. He, S. *et al.* Phase diagram and electronic indication of high-temperature superconductivity at 65 K in single-layer FeSe films. *Nat. Mater.* **12,** 605–610 (2013).
80. Lee, J. J. *et al.* Interfacial mode coupling as the origin of the enhancement of T_c in FeSe films on $SrTiO_3$. *Nature* **515,** 245–248 (2014).
81. Shiogai, J., Ito, Y., Mitsuhashi, T., Nojima, T. & Tsukazaki, A. Electric-field-induced superconductivity in electrochemically etched ultrathin FeSe films on $SrTiO_3$ and MgO. *Nat. Phys.* **12,** 42–46 (2015).
82. Lei, B. *et al.* Evolution of high-temperature superconductivity from a low-T_c phase tuned by carrier concentration in FeSe thin flakes. *Phys. Rev. Lett.* **116,** 077002 (2016).
83. Saito, Y. *et al.* Superconductivity protected by spin–valley locking in ion-gated MoS_2. *Nat. Phys.* **12,** 144–149 (2016).
84. Li, L. J. *et al.* Controlling many-body states by the electric-field effect in a two-dimensional material. *Nature* **529,** 185–189 (2015).
85. Bollinger, A. T. *et al.* Superconductor–insulator transition in $La_{2-x}Sr_xCuO_4$ at the pair quantum resistance. *Nature* **472,** 458–460 (2011).
86. Sherman, D. *et al.* The Higgs mode in disordered superconductors close to a quantum phase transition. *Nat. Phys.* **11,** 188–192 (2015).
87. Matsunaga, R. *et al.* Light-induced collective pseudospin precession resonating with Higgs mode in a superconductor. *Science* **345,** 1145–1149 (2014).
88. Nikuni, T., Oshikawa, M., Oosawa, A. & Tanaka, H. Bose–Einstein condensation of dilute magnons in $TlCuCl_3$. *Phys. Rev. Lett.* **84,** 5868–5871 (2000).
89. Giamarchi, T., Rüegg, C. & Tchernyshyov, O. Bose–Einstein condensation in magnetic insulators. *Nat. Phys.* **4,** 198–204 (2008).
90. Jaime, M. *et al.* Magnetic-field-induced condensation of triplons in Han purple pigment $BaCuSi_2O_6$. *Phys. Rev. Lett.* **93,** 087203 (2004).
91. Sebastian, S. E. *et al.* Dimensional reduction at a quantum critical point. *Nature* **441,** 617–620 (2006).
92. Kimura, S. *et al.* Ferroelectricity by Bose–Einstein condensation in a quantum magnet. *Nat. Commun.* **7,** 12822 (2016).
93. Demokritov, S. O. *et al.* Bose–Einstein condensation of quasi-equilibrium magnons at room temperature under pumping. *Nature* **443,** 430–433 (2006).
94. Bozhko, D. A. *et al.* Supercurrent in a room-temperature Bose-Einstein magnon condensate. *Nat. Phys.* **12,** 1057–1062 (2016).
95. Li, J. I. A., Taniguchi, T., Watanabe, K., Hone, J. & Dean, C. R. Excitonic superfluid phase in double bilayer graphene. *Nat. Phys.* **13,** 751–755 (2016).
96. Nandi, D., Finck, A. D. K., Eisenstein, J. P., Pfeiffer, L. N. & West, K. W. Exciton condensation and perfect Coulomb drag. *Nature* **488,** 481–484 (2012).
97. Fogler, M. M., Butov, L. V & Novoselov, K. S. High-temperature superfluidity with indirect excitons in van der Waals heterostructures. *Nat. Commun.* **5,** 4555 (2014).
98. Wu, F.-C., Xue, F. & MacDonald, A. H. Theory of two-dimensional spatially indirect equilibrium exciton condensates. *Phys. Rev. B* **92,** 165121 (2015).
99. Sun, Y. *et al.* Bose–Einstein condensation of long-lifetime polaritons in thermal equilibrium. *Phys. Rev. Lett.* **118,** 016602 (2017).
100. Cotleţ, O., Zeytinoğlu, S., Sigrist, M., Demler, E. & Imamoğlu, A. Superconductivity and other collective phenomena in a hybrid Bose–Fermi mixture formed by a polariton condensate and an electron system in two dimensions. *Phys. Rev. B* **93,** 054510 (2016).
101. McLeod, A. S. *et al.* Nanotextured phase coexistence in the correlated insulator V_2O_3. *Nat. Phys.* **13,** 80–86 (2016).
This paper shows that the insulator-to-metal transition in correlated oxides is associated with the phase separation at nano- and mesoscales.
102. Ma, E. Y. *et al.* Mobile metallic domain walls in an all-in-all-out magnetic insulator. *Science* **350,** 538–541 (2015).
103. Mitrano, M. *et al.* Possible light-induced superconductivity in K_3C_{60} at high temperature. *Nature* **530,** 461–464 (2016).
This work is the latest result from the group of A. Cavalleri on transient enhancement of superconducting pairing in unconventional superconductors.
104. Kennes, D. M., Wilner, E. Y., Reichman, D. R. & Millis, A. J. Transient superconductivity from electronic squeezing of optically pumped phonons. *Nat. Phys.* **13,** 479–483 (2017).
105. Spivak, B. & Kivelson, S. A. Transport in two dimensional electronic micro-emulsions. *J. Phys. IV France* **131,** 255–256 (2005).
106. Yamaura, J. *et al.* Tetrahedral Magnetic Order and the Metal-Insulator Transition in the Pyrochlore Lattice of $Cd_2Os_2O_7$. *Phys. Rev. Lett.* **108,** 247205 (2012).
107. Yamaji, Y. & Imada, M. Metallic interface emerging at magnetic domain wall of antiferromagnetic insulator: fate of extinct Weyl electrons. *Phys. Rev. X* **4,** 021035 (2014).
108. Yamaji, Y. & Imada, M. Modulated helical metals at magnetic domain walls of pyrochlore iridium oxides. *Phys. Rev. B* **93,** 195146 (2016).
109. Nakamura, F. *et al.* Electric-field-induced metal maintained by current of the Mott insulator Ca_2RuO_4. *Sci. Rep.* **3,** 2536 (2013).
110. Liu, M. K. *et al.* Photoinduced phase transitions by time-resolved far-infrared spectroscopy in V_2O_3. *Phys. Rev. Lett.* **107,** 066403 (2011).
111. Kübler, C. *et al.* Coherent structural dynamics and electronic correlations during an ultrafast insulator-to-metal phase transition in VO_2. *Phys. Rev. Lett.* **99,** 116401 (2007).
112. Rini, M. *et al.* Control of the electronic phase of a manganite by mode-selective vibrational excitation. *Nature* **449,** 72–74 (2007).
113. Beaud, P. *et al.* A time-dependent order parameter for ultrafast photoinduced phase transitions. *Nat. Mater.* **13,** 923–927 (2014).
114. Morrison, V. R. *et al.* A photoinduced metal-like phase of monoclinic VO_2 revealed by ultrafast electron diffraction. *Science* **346,** 445–448 (2014).
115. Han, T.-R. T. *et al.* Exploration of metastability and hidden phases in correlated electron crystals visualized by femtosecond optical doping and electron crystallography. *Sci. Adv.* **1**, e1400173 (2015).
116. Beaud, P. *et al.* Ultrafast structural phase transition driven by photoinduced melting of charge and orbital order. *Phys. Rev. Lett.* **103,** 155702 (2009).
117. Nova, T. F. *et al.* An effective magnetic field from optically driven phonons. *Nat. Phys.* **13,** 132–136 (2017).
118. Mankowsky, R. *et al.* Nonlinear lattice dynamics as a basis for enhanced superconductivity in $YBa_2Cu_3O_{6.5}$. *Nature* **516,** 71–73 (2014).
119. Babadi, M., Knap, M., Martin, I., Refael, G. & Demler, E. Theory of parametrically amplified electron–phonon superconductivity. *Phys. Rev. B* **96,** 014512 (2017).
120. Wegkamp, D. *et al.* Instantaneous band gap collapse in photoexcited monoclinic VO_2 due to photocarrier doping. *Phys. Rev. Lett.* **113,** 216401 (2014).
121. Popmintchev, T., Chen, M.-C., Arpin, P., Murnane, M. M. & Kapteyn, H. C. The attosecond nonlinear optics of bright coherent X-ray generation. *Nat. Photon.* **4,** 822–832 (2010).
122. Rybka, T. *et al.* Sub-cycle optical phase control of nanotunnelling in the single-electron regime. *Nat. Photon.* **10,** 667–670 (2016).
123. Moore, J. E. The birth of topological insulators A primer on topological insulators. *Nature* **464,** 194–198 (2010).
124. Jia, S., Xu, S.-Y. & Hasan, M. Z. Weyl semimetals, Fermi arcs and chiral anomalies. *Nat. Mater.* **15,** 1140–1144 (2016).
125. Yan, B. & Felser, C. Topological materials: Weyl semimetals. *Annu. Rev. Condens. Matter Phys* **8,** 337–354 (2017).
126. Hasan, M. Z. & Kane, C. L. Colloquium: Topological insulators. *Rev. Mod. Phys.* **82,** 3045–3067 (2010).

127. Beenakker, C. & Kouwenhoven, L. A road to reality with topological superconductors. *Nat. Phys.* **12,** 618–621 (2016).
128. Beenakker, C. W. J. Search for Majorana fermions in superconductors. *Annu. Rev. Condens. Matter Phys* **4,** 113–136 (2013).
129. Kitagawa, T., Oka, T., Brataas, A., Fu, L. & Demler, E. Transport properties of nonequilibrium systems under the application of light: Photoinduced quantum Hall insulators without Landau levels. *Phys. Rev. B* **84,** 235108 (2011).
130. Lindner, N. H., Bergman, D. L., Refael, G. & Galitski, V. Topological Floquet spectrum in three dimensions via a two-photon resonance. *Phys. Rev. B* **87,** 235131 (2013).
131. Qian, X., Liu, J., Fu, L. & Li, J. Quantum spin Hall effect in two-dimensional transition metal dichalcogenides. *Science* **346,** 1344–1347 (2014).
132. Fei, Z. *et al.* Edge conduction in monolayer WTe_2. *Nat. Phys.* **13,** 677–682 (2017).
133. Tang, S. *et al.* Quantum spin Hall state in monolayer 1T′-WTe_2. *Nat. Phys.* **13,** 683–687 (2017).
134. Yu, R. *et al.* Quantized anomalous Hall effect in magnetic topological insulators. *Science* **329,** 61–64 (2010).
135. Chang, C.-Z. *et al.* Experimental observation of the quantum anomalous Hall effect in a magnetic topological insulator. *Science* **340,** 167–170 (2013).
136. Ju, L. *et al.* Topological valley transport at bilayer graphene domain walls. *Nature* **520,** 650–655 (2015).
137. Sie, E. J. *et al.* Valley-selective optical Stark effect in monolayer WS_2. *Nat. Mater.* **14,** 290–294 (2015).
138. Xu, S.-Y. *et al.* Topological phase transition and texture inversion in a tunable topological insulator. *Science* **332,** 560–564 (2011).
139. Moll, P. J. W. *et al.* Transport evidence for Fermi-arc-mediated chirality transfer in the Dirac semimetal Cd_3As_2. *Nature* **535,** 266–270 (2016).
140. Hirschberger, M. *et al.* SI: The chiral anomaly and thermopower of Weyl fermions in the half-Heusler GdPtBi. *Nat. Mater.* **15,** 1161–1165 (2016).
141. Wan, X., Turner, A., Vishwanath, A. & Savrasov, S. Y. Electronic structure of pyrochlore iridates: From topological Dirac metal to Mott insulator. *Phys. Rev. B* **83,** 205101 (2011).
142. Xu, G., Weng, H., Wang, Z., Dai, X. & Fang, Z. Chern semimetal and the quantized anomalous Hall effect in $HgCr_2Se_4$. *Phys. Rev. Lett.* **107,** 186806 (2011).
143. Chang, G. *et al.* Room-temperature magnetic topological Weyl fermion and nodal line semimetal states in half-metallic Heusler Co_2TiX (X=Si, Ge, or Sn). *Sci. Rep.* **6,** 38839 (2016).
144. Wang, Z. *et al.* Time-reversal-breaking Weyl fermions in magnetic Heusler alloys. *Phys. Rev. Lett.* **117,** 236401 (2016).
145. Hübener, H., Sentef, M. A., De Giovannini, U., Kemper, A. F. & Rubio, A. Creating stable Floquet–Weyl semimetals by laser-driving of 3D Dirac materials. *Nat. Commun.* **8,** 13940 (2017).
146. Sentef, M. A. *et al.* Theory of Floquet band formation and local pseudospin textures in pump-probe photoemission of graphene. *Nat. Commun.* **6,** 7047 (2015).
147. Benito, M., Gómez-León, A., Bastidas, V. M., Brandes, T. & Platero, G. Floquet engineering of long-range *p*-wave superconductivity. *Phys. Rev. B* **90,** 205127 (2014).
148. Zhang, X.-X., Ong, T. T. & Nagaosa, N. Theory of photoinduced Floquet Weyl semimetal phases. *Phys. Rev. B* **94,** 235137 (2016).
149. Claassen, M., Jiang, H.-C., Moritz, B. & Devereaux, T. P. Dynamical time-reversal symmetry breaking and photo-induced chiral spin liquids in frustrated Mott insulators. Preprint at http://arxiv.org/abs/1611.07964 (2016).
150. Kumar, A. *et al.* Chiral plasmon in gapped Dirac systems. *Phys. Rev. B* **93,** 041413 (2016).
151. Karzig, T., Bardyn, C.-E., Lindner, N. H. & Refael, G. Topological polaritons. *Phys. Rev. X* **5,** 031001 (2015).
152. Giannetti, C. *et al.* Ultrafast optical spectroscopy of strongly correlated materials and high-temperature superconductors: a non-equilibrium approach. *Adv. Phys.* **65,** 58–238 (2016).
153. Wang, H. *et al.* Bright high-repetition-rate source of narrowband extreme-ultraviolet harmonics beyond 22 eV. *Nat. Commun.* **6,** 7459 (2015).
154. Elsaesser, T. & Woerner, M. Perspective: Structural dynamics in condensed matter mapped by femtosecond x-ray diffraction. *J. Chem. Phys.* **140,** 020901 (2014).
155. Zhao, L. *et al.* Evidence of an odd-parity hidden order in a spin-orbit coupled correlated iridate. *Nat. Phys.* **12,** 32–36 (2015).
156. Zhao, L. *et al.* A global inversion-symmetry-broken phase inside the pseudogap region of $YBa_2Cu_3O_y$. *Nat. Phys.* **13,** 250–254 (2017).
157. Harter, J., Zhao, Z. Y., Yan, J.-Q., Mandrus, D. G. & Hsieh, D. A parity-breaking electronic nematic phase transition in the spin-orbit coupled metal $Cd_2Re_2O_7$. *Science* **356,** 295–299 (2017).
158. Bowlan, P. *et al.* Probing and controlling terahertz-driven structural dynamics with surface sensitivity. *Optica* **4,** 383–387 (2017).
159. Dean, M. P. M. *et al.* Ultrafast energy- and momentum-resolved dynamics of magnetic correlations in the photo-doped Mott insulator Sr_2IrO_4. *Nat. Mater.* **15,** 601–605 (2016).
160. Abreu, E. *et al.* Dynamic conductivity scaling in photoexcited V_2O_3 thin films. *Phys. Rev. B* **92,** 085130 (2015).
161. Ni, G. X. *et al.* Ultrafast optical switching of infrared plasmon polaritons in high-mobility graphene. *Nat. Photon.* **10,** 244–247 (2016).
162. Dönges, S. A. *et al.* Ultrafast nanoimaging of the photoinduced phase transition dynamics in VO_2. *Nano Lett.* **16,** 3029–3035 (2016).
163. Eisele, M. *et al.* Ultrafast multi-terahertz nano-spectroscopy with sub-cycle temporal resolution. *Nat. Photon.* **8,** 841–845 (2014).
164. Weiner, A. Femtosecond pulse shaping using spatial light modulators. *Rev. Sci. Instrum.* **71,** 1929–1960 (2000).
165. Yusupov, R. *et al.* Coherent dynamics of macroscopic electronic order through a symmetry breaking transition. *Nat. Phys.* **6,** 681–684 (2010).
166. Martin, I., Refael, G. & Halperin, B. Topological frequency conversion in strongly driven quantum systems. Preprint at http://arxiv.org/abs/1612.02143v1 (2016).
167. Cundiff, S. T. & Mukamel, S. Optical multidimensional coherent spectroscopy. *Phys. Today* **66,** 44–49 (July, 2013).
168. Riek, C. *et al.* Direct sampling of electric-field vacuum fluctuations. *Science* **350,** 420–423 (2015).
169. Antonius, G. & Louie, S. G. Temperature-induced topological phase transitions: promoted versus suppressed nontrivial topology. *Phys. Rev. Lett.* **117,** 246401 (2016).
170. Aoki, H. *et al.* Nonequilibrium dynamical mean-field theory and its applications. *Rev. Mod. Phys.* **86,** 779–837 (2014).
171. Das Sarma, S., Freedman, M. & Nayak, C. Majorana zero modes and topological quantum computation. *npj Quant. Inf.* **1,** 15001 (2015).
172. Bradlyn, B. *et al.* Beyond Dirac and Weyl fermions: Unconventional quasiparticles in conventional crystals. *Science* **353,** aaf5037 (2016).
173. Zhang, J. *et al.* Observation of a discrete time crystal. *Nature* **543,** 217–220 (2017).
174. Choi, S. *et al.* Observation of discrete time-crystalline order in a disordered dipolar many-body system. *Nature* **543,** 221–225 (2017).

Acknowledgments

Research at Columbia is supported by DE-FG02-00ER45799 (fundamental physics of graphene), NSF DMR1609096 (high-T_c superconductivity), ARO-W911NF-17-1-0543 (correlated oxides), AFOSR FA9550-15-1-0478 (van der Waals heterostructures), ONR N00014-15-1-2671 (graphene-based devices) and NSF-EFRI EFMA 1741660 (topological effects in graphene). D.N.B. is the Gordon and Betty Moore Foundation's EPiQS Initiative Investigator through Grant GBMF4533. Additionally, research at Columbia and UCSD is supported by DE-SC0018218 (ultrafast electrodynamics of superconductors) and DE-SC0012375 (ultrafast dynamics of oxides). Research at Caltech is supported by ARO W911NF-17-1-0204 (hidden order in correlated materials), DOE DE-SC0010533 (topological superconductors). D.H. acknowledges support from the David and Lucile Packard Foundation and the Institute for Quantum Information and Matter, an NSF Physics Frontier Center (PHY-1125565) with support of the Gordon and Betty Moore Foundation (GBMF1250). Additionally, research at Caltech and UCSD is supported by ARO W911NF-16-1-0361 (Floquet engineering and metastable states).

Additional information

Reprints and permissions information is available online at www.nature.com/reprints. Correspondence and requests for materials should be addressed to D.N.B., R.D.A. or D.H.

Competing financial interests

The authors declare no competing financial interests.